

# Pd-Pt/modified GO as an efficient and selective heterogeneous catalyst for the reduction of nitroaromatic compounds to amino aromatic compounds by the hydrogen source

Hossein Salahshournia | Mehran Ghiaci

Department of Chemistry, Isfahan University of Technology, Isfahan 8415683111, Iran

## Correspondence

Mehran Ghiaci, Department of Chemistry, Isfahan University of Technology, Isfahan, 8415683111, Iran.  
Email: mghiaci@cc.iut.ac.ir

## Funding information

Isfahan University of Technology; Karoun Petrochemical Company

In this work, different nitroaromatic compounds were successfully reduced to their corresponding aromatic amines with excellent conversion and selectivity in methanol at 50 °C by using Pd-Pt nanoparticles immobilized on the modified graphene oxide (*m*-GO) and hydrogen as the reducing source. The catalytic efficiency of Pd and Pd-Pt loading on the modified GO was investigated for the reduction of various nitroaromatic compounds, and the Pd-Pt/*m*-GO system demonstrated the highest conversion and selectivity. The catalyst was characterized by different techniques including FT-IR, Raman, UV-Vis, XRD, BET, XPS, FESEM, EDS, and TEM. The metal nanoparticles with the size of less than 10 nm were uniformly distributed on the *m*-GO. The catalyst could be reused at least five times without losing activity, showing the stability of the catalyst structure. Finally, the efficiency of the prepared catalyst was compared with Pd-Pt/AC, and Pd-Pt/GO catalysts.

## KEYWORDS

diisocyanate, heterogenous catalyst, hydrogenation, modified graphene oxide, Pd and Pt supported catalyst

## 1 | INTRODUCTION

Aromatic amines are important raw materials, especially for the production of phenyl isocyanates,<sup>[1]</sup> additives for rubber industries,<sup>[2]</sup> dyes and pigments,<sup>[3,4]</sup> pesticides,<sup>[5,6]</sup> etc. The catalytic hydrogenation of nitro aromatics, which can be performed in the gas or liquid phase due to its environmentally friendly nature, is one of the best methods for the manufacture of aromatic amines.<sup>[7,8]</sup> In this respect, different metal supported catalysts have been designed for the hydrogenation of nitro aromatic compounds.<sup>[9,10]</sup> Various metals including Pd,<sup>[11]</sup> Pt,<sup>[12]</sup> Ni,<sup>[13]</sup> Ru,<sup>[14]</sup> and Cu<sup>[15]</sup> are applied for this reduction;

different parameters such as the type of metal, the size of the metal particles,<sup>[16]</sup> the support,<sup>[16]</sup> the solvent,<sup>[17]</sup> and hydrogen pressure<sup>[18]</sup> are very important factors in this catalytic reaction. Among the mentioned metals, Pt and Pd supported catalysts are the most effective catalysts in the liquid-phase hydrogenation; showing the desirable activity and selectivity.<sup>[19,20]</sup> In terms of industrial applications, the catalyst support not only affects its catalytic activity, but also influences its longevity and recovery from the reaction mixture. The main concern in choosing a specific support is, perhaps, geometrical effects which can prevent the aggregation of metal nanoparticles. It is known that the interaction between nano-sized metals

and metal oxide type supports can lead to the desirable catalytic performance.<sup>[21]</sup> Also, one of the best supports, especially for palladium or platinum, has been activated carbon. Therefore, a combination of these can make it possible to apply graphene oxide as a support, which might be beneficial. In recent years, much research has been done on graphene and graphene oxide due to their unique structures.<sup>[22,23]</sup> Especially, in catalytic applications, in addition to effective catalytic components, these materials usually exhibit synergistic contributions to the catalytic reactions.<sup>[24,25]</sup>

In this work, in the continuation of our previous research interests, we designed a new catalyst, Pd-Pt/*m*-GO, in which the three-dimensional *m*-GO acted as the support for immobilizing palladium and platinum nanoparticles. The prepared composite was characterized by FT-IR, Raman, X-ray diffraction, BET, TEM, FESEM and X-ray photoelectron spectroscopy (XPS). The catalytic performance of the Pd-Pt/*m*-GO for the liquid-phase reduction of various nitroaromatic compounds was investigated using a hydrogen source, with focus on stability of the catalyst.

## 2 | EXPERIMENTAL SECTION

### 2.1 | Materials and techniques

The reactor used for the hydrogenation reactions was a stainless steel Bochiglasuster-type hydrogenation reactor, model cyclone 075, with the capacity of 300 ml, the maximum pressure of 60 bar and the temperature of 250 °C. Toluene diisocyanate (TDI) was a mixture of the 2,4- and 2,6- isomers (80:20) with the purity of at least 99.5%, as purchased from Karun Petrochemical Company (KRNPC). Other chemicals including PdCl<sub>2</sub> and K<sub>2</sub>PtCl<sub>6</sub>, graphite, and all of the solvents, such as dichloromethane (DCM), dimethyl formaldehyde (DMF) and methanol (MeOH), were purchased from Sigma-Aldrich. DMF preliminary was dried over MgSO<sub>4</sub>; then, it was distilled under vacuum over NaH. Graphene oxide was prepared from purified graphite by the Hummers method.<sup>[23]</sup>

A VARIAN gas chromatograph, model CP-3800, equipped with an FID detector was used for monitoring the reactions. The column was a Varian capillary column (CP-Sil 5 CB, 30 m 0.32 mm 0.25 μm). The initial temperature (100 to 280 °C with the rate 7.5 °C/min) was held at 280 °C for 15 min and the total time was 40.33 min. The products of the reduction reactions were identified by the GC/MS instrument (Fisons instrument 8060, USA). FESEM micrographs were obtained from the Scanning Electron Microscope (Mira 3-XMU FESEM, Germany). Particle size and morphology were determined from

TEM images obtained in the Philips CM-120 transmission electron microscope with the accelerator voltage of 100 KV (Germany). BET specific surface area and pore size distribution were measured on a PHS-1020 (PHS, China) system from the nitrogen adsorption-desorption isotherms at 77 K. FT-IR spectra were collected from a potassium bromide (KBr) pellet in a Jasco-680 plus spectrophotometer (Japan).

### 2.2 | Preparation of GO

Graphene oxide was prepared from graphite by the Hummers method.<sup>[23]</sup>

### 2.3 | Preparation of the modified graphene oxide with diisocyanate (*m*-GO)

In a typical procedure, a 100 ml round bottom flask was loaded with 500 mg graphene oxide and 50 ml of anhydrous dimethyl formaldehyde (DMF); then, the mixture was stirred for 15 min under nitrogen gas. Subsequently, 20 mmol toluene diisocyanate (TDI) was added and stirred under nitrogen gas for 24 hrs. Then, the reaction mixture was poured into 200 ml of methylene chloride, filtered and thoroughly washed with 50 ml of methylene chloride; and finally, the solid was dried under vacuum.

### 2.4 | Synthesis of the Pd-Pt/*m*-GO catalysts

In a typical procedure, 37.2 mg of PdCl<sub>2</sub> and 7.9 mg of K<sub>2</sub>PtCl<sub>6</sub> were dissolved in 5 ml of deionized water and stirred for 30 min. 500 mg of the modified graphene oxide with toluene diisocyanate (*m*-GO) was dispersed in 10 ml of ethanol; then the aqueous solution containing palladium and platinum salts was added to the mixture and sonicated (2 × 15 min). The mixture was refluxed for 10 hr at 80 °C. Then sodium carbonate (100 mg) was added and the mixture was refluxed for 2 hr (pH reached to 8). At this step, palladium hydroxide and platinum hydroxide were immobilized on the *m*-GO. The solid was filtered and thoroughly washed with deionized water and dried at 60 °C. Finally, the palladium and platinum hydroxides immobilized on *m*-GO were reduced by hydrogen at 50 °C for 2 hr. The prepared catalyst contained 5 wt% palladium and platinum, with a ratio of 7 to 1 (calculations are shown in the supplementary data).

## 2.5 | Hydrogenation of 2,4-dinitrotoluene

To carry out the hydrogenation reaction of 2,4-dinitrotoluene, the stainless steel Bochiglasuster hydrogenation reactor was initially washed several times with deionized water and finally with methanol. The catalyst (100 mg) was loaded into the reactor and the catalyst was refreshed under hydrogen gas for 2 hr at 50 °C before the reaction. Then the reactor was charged with 2,4-dinitrotoluene (5000 mg) and 150 ml methanol. The reaction mixture was perched with N<sub>2</sub> (5 times); then, with H<sub>2</sub> gas, the hydrogen pressure was increased to 0.2 MPa. The reaction temperature was raised to 50 °C and the reaction mixture was stirred (1250 rpm). After the completion of the reaction, the catalyst was removed by filtration; then, the solvent was distilled under vacuum. The residue was dissolved in CH<sub>2</sub>Cl<sub>2</sub> and the progress of the reaction was checked by gas chromatography (Scheme 1).

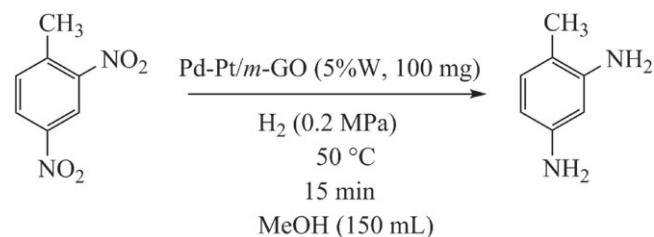
## 3 | RESULTS AND DISCUSSION

In this work, the Pd-Pt/*m*-GO was designed and its preparation is schematically demonstrated in Scheme 2. GO, toluene diisocyanate, PdCl<sub>2</sub>, and K<sub>2</sub>PtCl<sub>6</sub> were applied as the starting materials for the synthesis of the Pd-Pt/*m*-GO composite. The modified graphene oxide was first prepared through the reaction between GO and toluene diisocyanate in DMF, which was then dispersed in a PdCl<sub>2</sub>, and K<sub>2</sub>PtCl<sub>6</sub> aqueous solution; this was followed by adding Na<sub>2</sub>CO<sub>3</sub> for obtaining the Pd(OH)<sub>2</sub>-Pt(OH)<sub>2</sub>/*m*-GO composite. Finally, it was reduced by the hydrogen gas to obtain the Pd-Pt/*m*-GO composite.

### 3.1 | Characterization of the Pd-Pt/*m*-GO

#### 3.1.1 | XRD analysis

Figure 1 shows the XRD patterns of GO, *m*-GO, and Pd-Pt/*m*-GO composite. In the XRD pattern of graphene oxide, the peaks appeared at 11.9°, and 9.0°, demonstrating the layered structure of graphene oxide with the inter-layer spacing in the range of 7.4–9.8 Å. By the modification of the GO with toluene diisocyanate, these



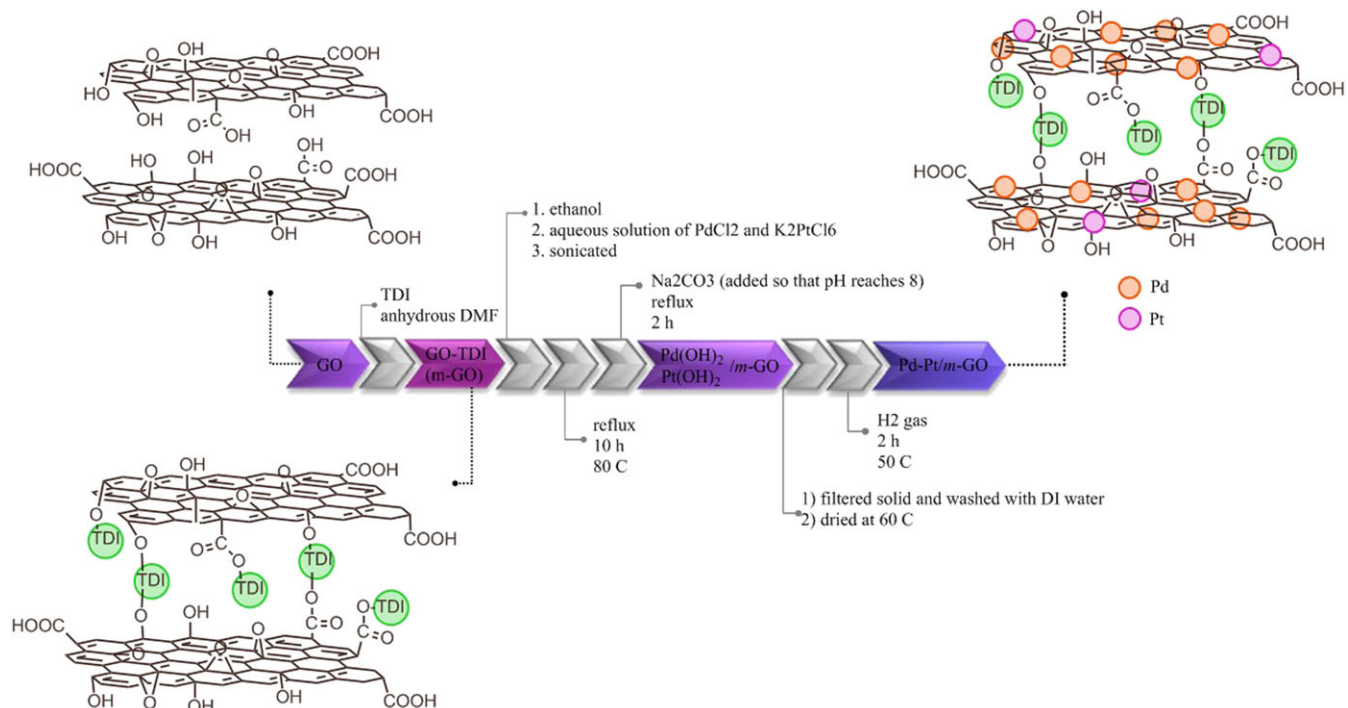
**SCHEME 1** Reduction of 2,4-dinitrotoluene

peaks were shifted to the lower 2θ, and a broad peak was also appeared at about 20°, showing that the inter-layer distances had been increased with a large distortion in the layered structure of GO.<sup>[26]</sup> In this process, one might expect that by the reaction between toluene diisocyanate and some of the hydroxyl groups present on the faces and edges of GO, not only the distance between the GO layers could be increased through crosslinking reactions, but also the morphology of the modified GO would be changed appreciably. The XRD patterns of Pd (JCPDS card no. 01–1310) and Pt (JCPDS card no. 87–0642) show common peaks at 39.7° (111), 45.9° (200) and 66.9° (220) where in the XRD pattern of the Pd-Pt/*m*-GO composite (Figure 1) these peaks can also be seen.<sup>[27–29]</sup> The appeared peaks indicate the presence of palladium and platinum in the prepared Pd-Pt/*m*-GO composite.<sup>[26]</sup>

#### 3.1.2 | TEM images, FESEM and EDS analysis

The morphology of the prepared catalyst, i.e., Pd-Pt/*m*-GO, was investigated by TEM and FESEM images. Figure 2a-b shows the TEM images of the Pd-Pt/*m*-GO catalyst with the distribution of Pd and Pt nanoparticles on the support, where the majority of the nanoparticles were congregated into large particles. The histograms of the particle size distribution of the catalyst showed that the mean diameter of Pd and Pt nanoparticles was in the range of 10 nm; based on EDS analysis, the ratio of Pd:Pt nanoparticles was about 3.14:1 that indicates the preference of Pt to accumulate at the surface. Also, it should be mentioned that ICP analysis has measured the ratio of Pd:Pt equal to 6:1 which was different from the ratio of the two metals used in the procedure proposed for the synthesis of the catalyst that we think part of palladium was leached during the work-up.

FESEM images shown in Figure 3 demonstrated the changes in the morphology of graphene oxide after treating with toluene diisocyanate as the linker between the graphene oxide sheets. The stacked sheets of graphene oxide (Figure 3a) through the reaction of diisocyanate with the hydroxyl groups present on the edges of the sheets were bended, and a more compact structure was obtained (Figure 3b). Of course, according to the XRD data, some of the diisocyanate penetrated into graphene oxide layers, increasing the inter-layer distances. Composite morphology after the immobilization of palladium and platinum nanoparticles showed that these nanoparticles were mainly on the surface of modified graphene oxide (Figure 3c-d).



**SCHEME 2** Schematic preparation of the Pd-Pt/*m*-GO catalyst

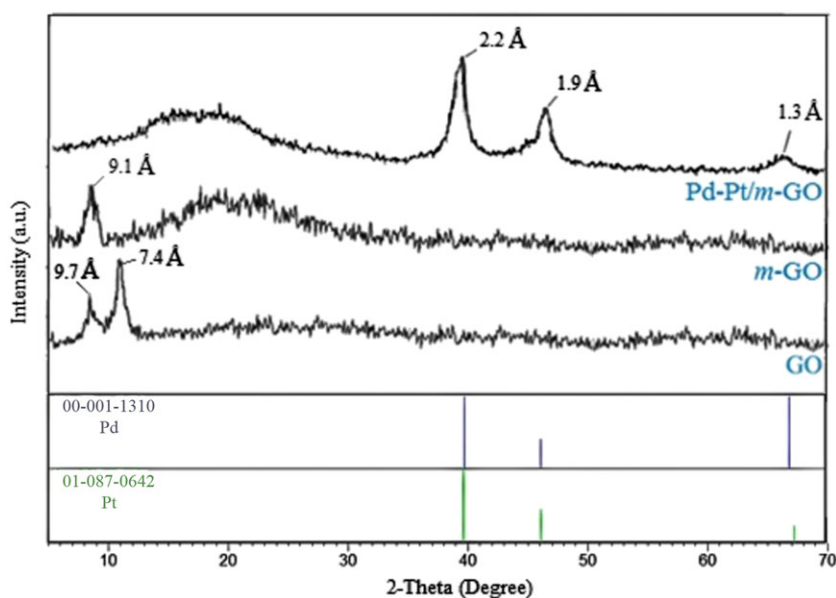


**FIGURE 1** XRD analysis of GO, *m*-GO and Pd-Pt/*m*-GO structures

### 3.1.3 | RAMAN spectroscopy

The Raman spectra of GO, *m*-GO and Pd-Pt/*m*-GO are compared in Figure 4. The G-band and D-band of the graphene oxide before modification appeared at 1590 cm<sup>-1</sup> and 1280 cm<sup>-1</sup>, respectively.<sup>[30]</sup> The D-band peak could be attributed to the amorphous carbon, as well

as the structural defects.<sup>[30]</sup> As shown, the intensity of this band was decreased when the graphene oxide was modified with diisocyanate. The peak observed at 2100 cm<sup>-1</sup> region (D'-peak) in both *m*-GO and Pd-Pt/*m*-GO could be related to irregularities that happened through modification. The peak appeared at 2600 cm<sup>-1</sup> in the Raman spectrum of Pd-Pt/*m*-GO was related to the Overton or



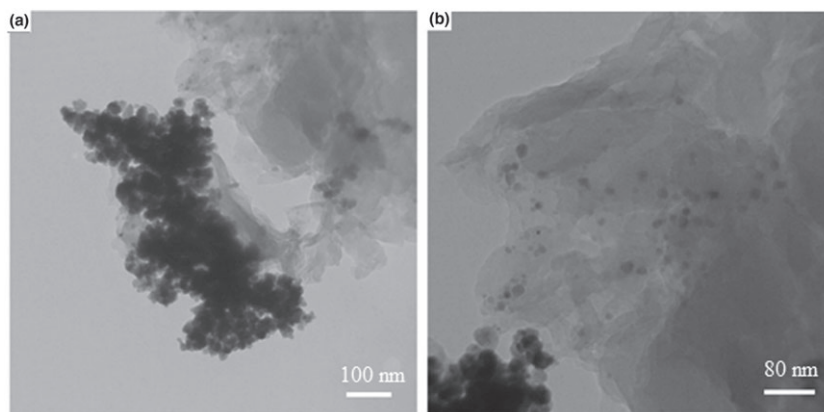


**FIGURE 2** TEM images of Pd-Pt/*m*-GO

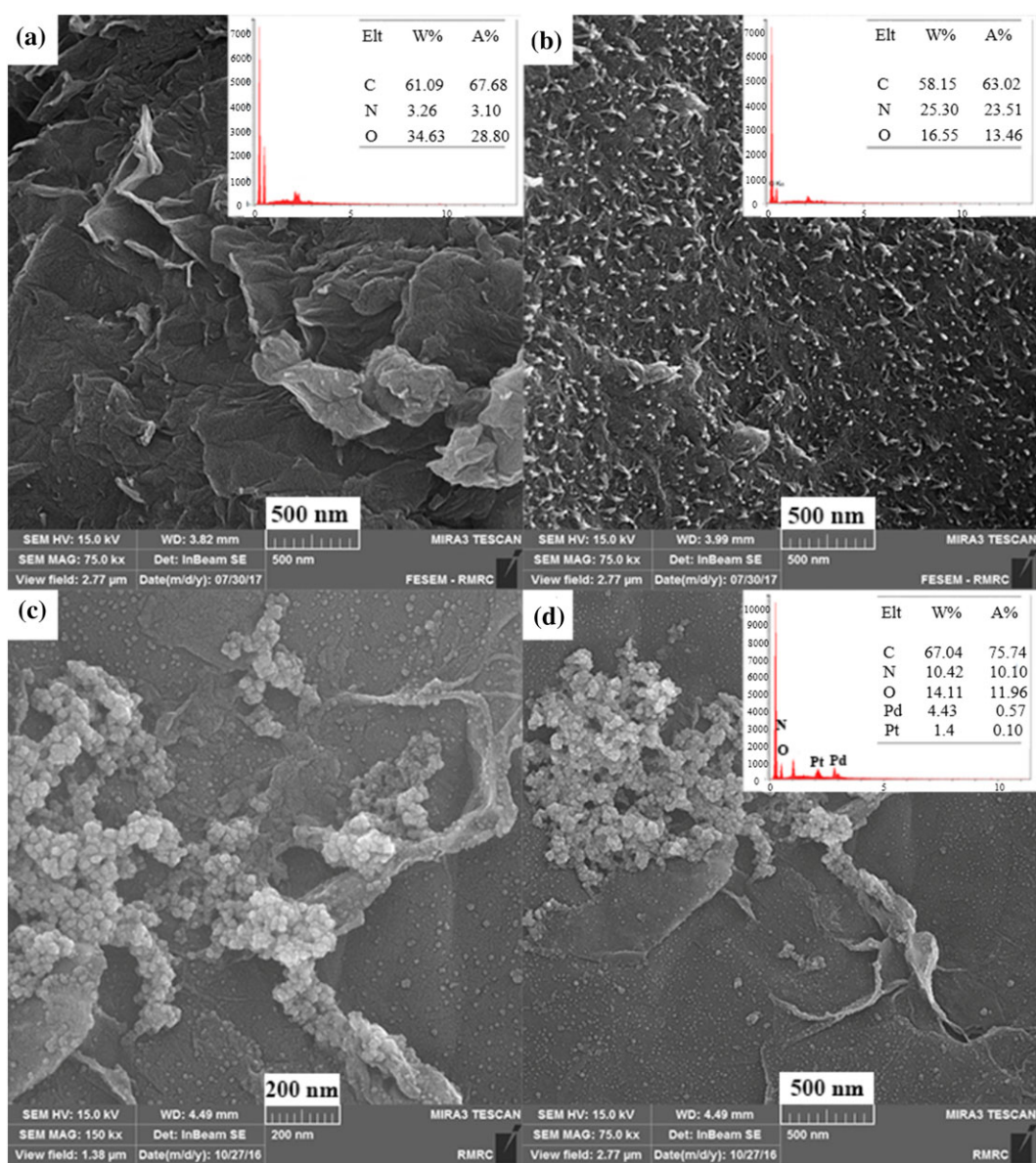


**FIGURE 3** FESEM images of GO, *m*-GO and Pd-Pt/*m*-GO structures

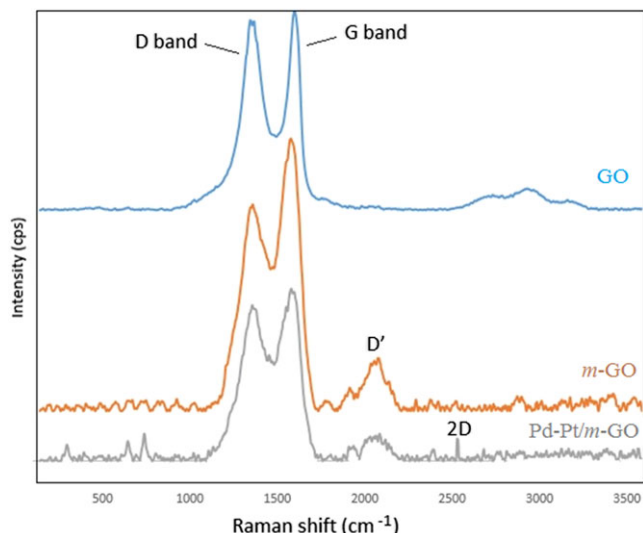


FIGURE 4 Raman spectra of GO, *m*-GO and Pd-Pt/*m*-GO

the second-order harmonic of D-band (2D band).<sup>[31,32]</sup> The 2D band represented the presence of order in a wide range of matter and emanated from a second-order diffusion process.<sup>[31]</sup> Also, the peaks that appeared at the 600–800  $\text{cm}^{-1}$  range were related to the presence of palladium and platinum metals in the composite.<sup>[33]</sup>

### 3.1.4 | BET analysis

Specific surface area of *m*-GO was 58  $\text{m}^2/\text{g}$ ; by adding nanometal particles, the surface area was decreased to 31  $\text{m}^2/\text{g}$ , which was reasonable. The pore distribution of the *m*-GO even after the immobilization of

nanoparticles showed that the pores were mainly in the range of 2–100 nm (the average pore diameter of 2.5 nm). The mesoporosity of the Pd-Pt/*m*-GO catalyst made most of the active sites accessible for reactant molecules; in the other words, it decreased the diffusion limitations for the reactant and the product. Moreover, by the modification of graphene oxide, as expected, the pore volume was increased from 0.163  $\text{cm}^3/\text{g}$  to 0.175  $\text{cm}^3/\text{g}$  (Figure 5).

### 3.1.5 | X-ray photoelectron spectroscopy (XPS) analysis

As shown in Figure 6, according to the XPS spectra, the surface chemical composition and the oxidation state of the elements were studied. The obtained survey XPS spectrum (Figure S1) of the Pd-Pt/*m*-GO catalyst demonstrated the presence of carbon, oxygen, nitrogen, palladium and platinum as the constructing elements. The high resolution spectra of C 1 s, O 1 s (Figure S2) showed the recognizable functional groups expected in the catalyst. In the XPS spectrum of N 1 s in Figure 6, there was one peak at 399.69 (399.45) eV, which was related to the ROCO-NH carbamate groups<sup>[31]</sup> produced through the reaction between the hydroxyl groups on GO with the isocyanate groups. The Pd 3d and Pt 4f deconvoluted spectra were fitted to two sets of doublets, the doublets with the binding energies of 335.38 and 340.65 eV were related to  $3d_{5/2}$  and  $3d_{3/2}$  transitions of  $\text{Pd}^0$ , respectively; while the other doublets, i.e., 336.69 and 341.88 eV, were attributed to  $\text{Pd}^{2+}$  in  $\text{Pd}(\text{OH})_2$ . Also, the doublets with the binding energies of 71. eV and 74.37 eV belonged to  $4f_{7/2}$  and  $4f_{7/2}$  of  $\text{Pt}^0$  and the

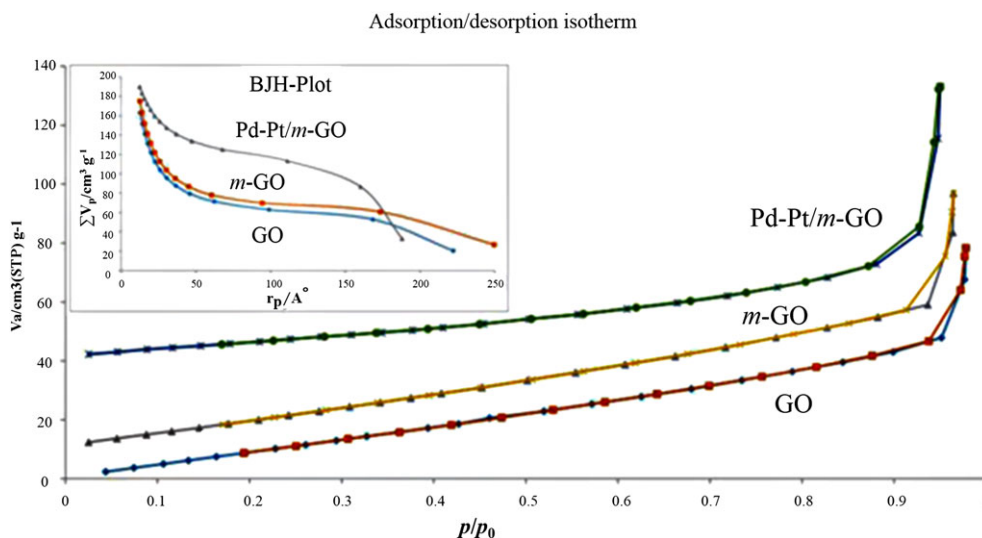
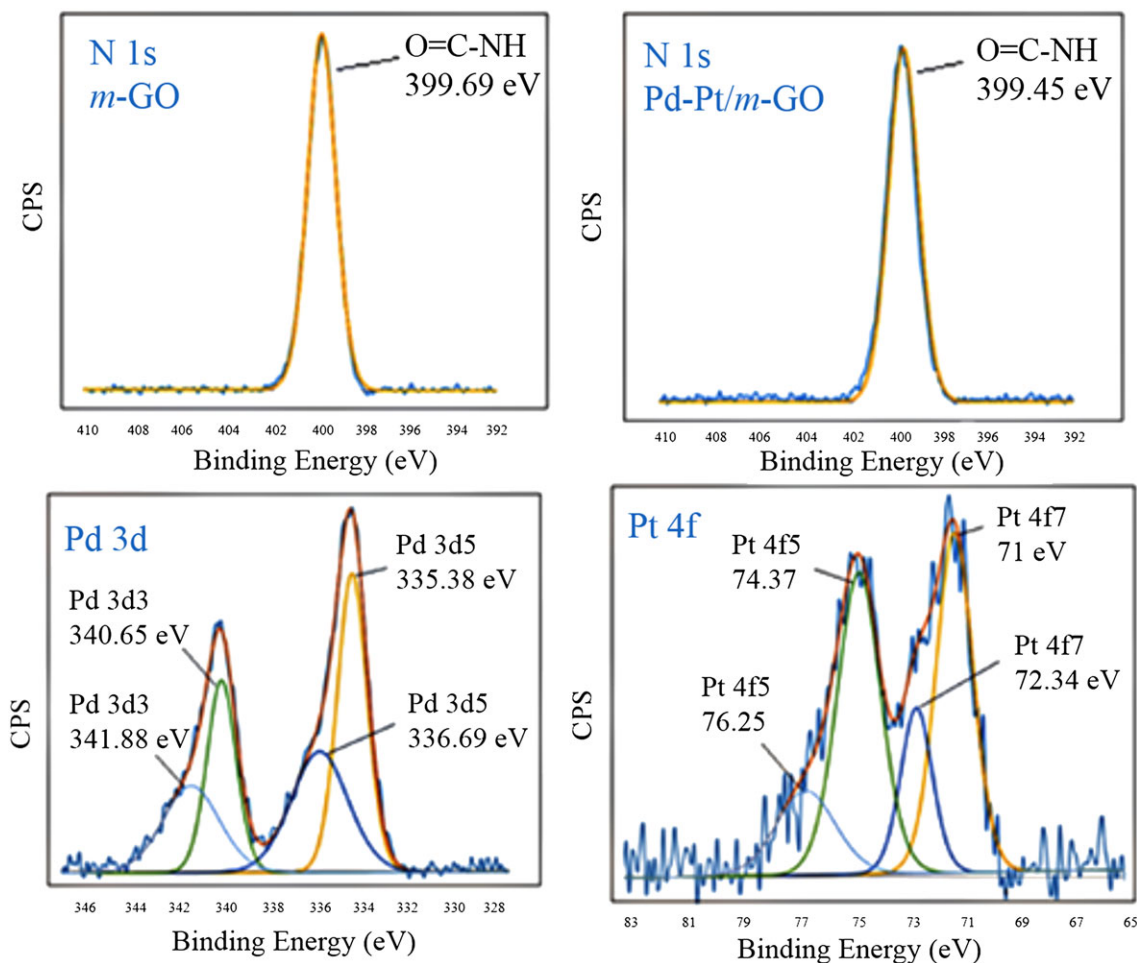


FIGURE 5 Nitrogen physisorption isotherms of GO, *m*-GO and Pd-Pt/*m*-GO



**FIGURE 6** N1 s, Pd 3d and Pt 4f XPS spectra of *m*-GO and Pd-Pt/*m*-GO

doublets at 72.34 and 76.25 eV were related to the remaining Pt (OH)<sub>2</sub> in the catalyst. Moreover, according to the XPS data (Table S1), palladium and platinum had 1.47%, and 0.15% atomic percent, respectively.

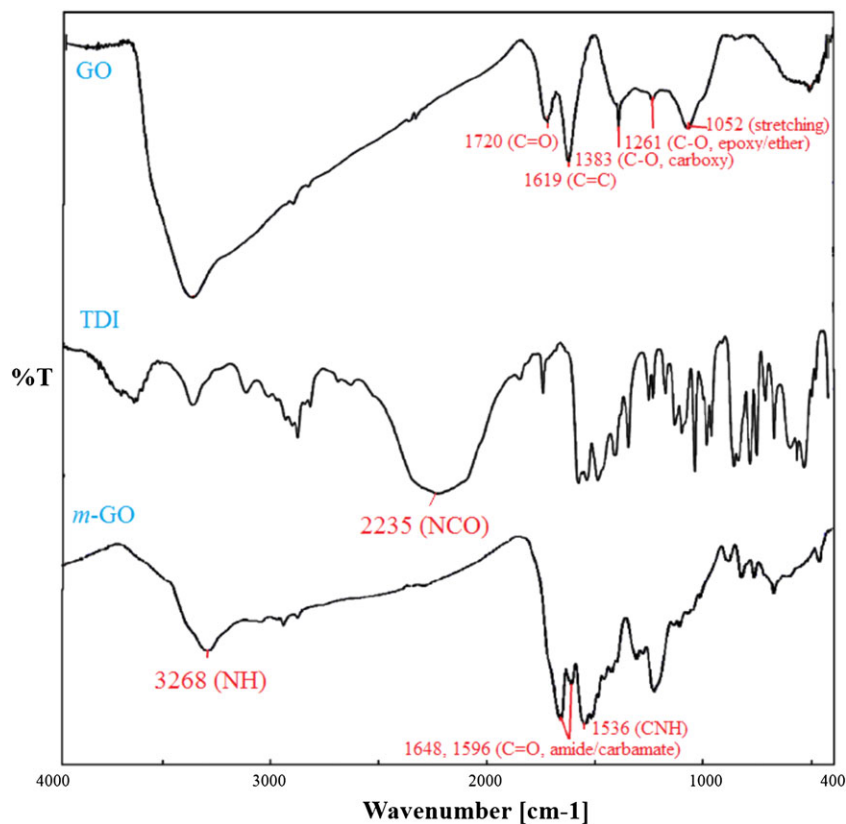
### 3.1.6 | FTIR spectra analysis

Figure 7 shows the changes that occurred in the FTIR spectrum of GO when modified with toluene isocyanate. The IR spectrum of the graphene oxide showed vibrational bands in the range of 1052–1380 cm<sup>-1</sup> which could be attributed to C-O alkoxide, epoxy/ether and hydroxyl groups vibrations; also, the OH stretching appeared as a broad peak at 2500–3400 cm<sup>-1</sup>. The presence of the carbon network with the sp<sup>2</sup> hybrid in the graphene-oxide skeleton revealed a band at the 1619 cm<sup>-1</sup> region. The peak that appeared at 1720 cm<sup>-1</sup> was related to the stretching vibration of C=O in the carboxyl groups present in the GO. Formation of the carbamate groups between the sheets, especially on the edges of GO, could

be easily detected by comparing the FTIR spectrum of graphene oxide before and after modification with toluene diisocyanate (TDI). After the entrance of TDI fragments in the GO, the band at 2235 cm<sup>-1</sup> which belonged to the isocyanate group in TDI was disappeared, and new bands related to the carbamate groups at 1648–1596 cm<sup>-1</sup> were observed; the changes that had happened in the region of 3400–2500 cm<sup>-1</sup> were consistent.

### 3.2 | Catalyst performance

Comparing the activated carbon (AC), *m*-GO, and GO as supports for expensive noble metals such as palladium and platinum might be interesting. Activated carbon (Norit SX plus cat) has a very high surface area (1000 m<sup>2</sup>/g), when *m*-GO, and GO have small surface areas 58 m<sup>2</sup>/g and 32 m<sup>2</sup>/g, respectively. What other factors do affect stability and performance of these catalysts? Do the functional groups such as carboxyl,



**FIGURE 7** FTIR spectra of GO, TDI and *m*-GO

hydroxyl, and carbamate exist in GO and/or *m*-GO could stabilize the metal nanoparticles or interaction between active sites of metal nanoparticles through their empty orbitals with the HOMO molecular orbital electrons of the activated carbon play a significant role in stability of these catalysts? The performance of the optimized catalyst Pd-Pt/*m*-GO in comparison with Pd-Pt/GO, and Pd-Pt/AC for reduction of various nitroaromatic compounds was examined in a stainless steel Bochiglasuster hydrogenation reactor in methanol at 323 K. The results of the conversion and selectivity to amino aromatic compounds are demonstrated in section 3.2.5. The conversion of the reactions was monitored by Gas chromatography, and the resulting products were identified by GC-Mass.

### 3.2.1 | Effect of loading of palladium and platinum on *m*-GO

To study the effect of metals and their synergistic effects on the reaction, reduction on the model nitroaromatic compound, i.e., 2,4-dinitrotoluene, was carried out at 323 K,  $P_{H_2} = 0.2$  MPa, 100 mg catalyst, and for 15 min. The results are summarized in Table 1. As can be seen, the catalyst with 4.4 wt% and 5 wt% palladium on the *m*-GO could not complete the reaction, and the

**TABLE 1** Loading of Pd/Pt on the modified GO

Entry	Catalyst	Conversion (%)	Selectivity (%)	TOF ( $h^{-1}$ )
1	Blank	–	–	–
2	GO	–	–	–
3	<i>m</i> -GO	–	–	–
4	5 wt% (only Pd)	82	100	1888
5	4.4 wt% (only Pd)	71	100	1856
6	0.6 wt% (only Pt)	6	100	2105
7	3 wt%*	40	100	1800
8	5 wt%*	100	100	2700
9	8 wt%*	100	100	1687

Reaction Conditions: 2,4-dinitrotoluene (5000 mg), catalyst (100 mg),  $CH_3OH$  (solvent) = 150 ml,  $P_{H_2} = 0.2$  MPa,  $t = 15$  min,  $T = 50$  °C

\*Ratio of Pd/Pt was 7:1

conversion was 71% and 82%, respectively. By using a catalyst containing just Pt (0.6 wt%) the conversion of the reaction was only 6% (entry 6). However, by adding 5–20 wt% platinum (relative to Pd), we were able to conduct the reduction quantitatively when a ratio of 7:1 of Pd:Pt was used for the preparation of the Pd-Pt/*m*-GO catalyst.



**TABLE 2** Amount of catalyst (5% Pd-Pt/*m*-GO)

Entry	Catalyst (mg)	Conversion (%)	Selectivity (%)	TOF (h <sup>-1</sup> )
1	40	22	100	1485
2	60*	51	100	2295
3	80**	73	100	2463
4	100	100	100	2700
5	120	100	100	2250
6	170	100	100	1593

Reaction conditions: Substrate (5000 mg), CH<sub>3</sub>OH = 150 ml, *t* = 15 min, P<sub>H<sub>2</sub></sub> = 0.2 MPa, *T* = 50 °C

\*After 1 hr, the yield was 57%;

\*\*yield of the reaction was 94% after 1 hr.

### 3.2.2 | Amount of the catalyst (5% wt Pd-Pt/*m*-GO)

To optimize the effect of the amount of the Pd-Pt/*m*-GO catalyst, the reduction reaction was conducted using different amounts of the catalyst (Table 2). As shown, the 100 mg catalyst was enough to complete the reaction with the selectivity of 100% in 15 min.

### 3.2.3 | Effect of temperature

The catalytic activity of the Pd-Pt/*m*-GO was studied as a function of temperature. Table 3 demonstrates the results of the reduction of 2,4-dinitro toluene at 20, 30, 40, 50, 60, and 70 °C. As can be seen, the reaction temperature had a significant influence on the completion of the reaction. By increasing the temperature to 50 °C, the reaction was completed in 15 min with 100% selectivity.

**TABLE 3** Effect of temperature

Entry	T (°C)	Time (min)	Yield (%)	TOF(h <sup>-1</sup> )
1	20	15	10	270
2	30	15	56	1512
3	40	15	88	2376
4	50	15	100	2700
5	60	15	100	2700
6	70	15	100	2700

Reaction Conditions: 2,4-dinitrotoluene (5000 mg), catalyst (100 mg), CH<sub>3</sub>OH (solvent) = 150 ml, P<sub>H<sub>2</sub></sub> = 0.2 MPa

**TABLE 4** Effect of the pressure of hydrogen

Entry	H <sub>2</sub> Pressure (MPa)	Time (min)	Yield (%)	TOF (h <sup>-1</sup> )
1	0.1	15	-	-
2	0.15	15	55	1485
3	0.2	15	100	2700
4	0.25	15	100	2700
5	0.3	15	100	2700

Reaction Conditions: 2,4-dinitrotoluene (5000 mg), catalyst (100 mg), CH<sub>3</sub>OH (Solvent) = 150 ml

### 3.2.4 | Effect of pressure of hydrogen and solvent

Table 4 demonstrates the effect of different pressures of hydrogen on the reduction of 2,4-dinitrotoluene over the Pd-Pt/*m*-GO catalyst. The results showed that when the pressure of hydrogen was reached to 0.2 MPa, the conversion and selectivity were increased to 100%. Moreover, the reaction was carried out in different solvents such as acetic acid, ethanol, methanol, and dichloromethane, where the methanol was chosen as the best solvent (Table 5).

### 3.2.5 | Reduction of other nitro-aromatic compounds

The reduction of various nitro arene derivatives was carried out in the optimized conditions obtained for the reduction of 2,4-dinitrotoluene. The results are summarized in Table 6. As shown, various nitro arene derivatives were reduced using this catalyst, and prepare the related products with a very good yield and selectivity.

### 3.2.6 | Reusability of catalyst

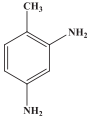
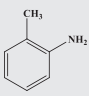
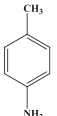
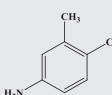
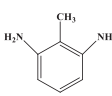
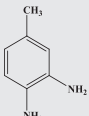
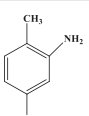
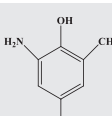
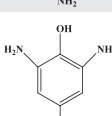
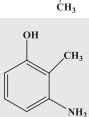
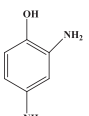
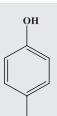
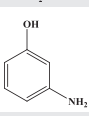
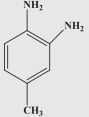
The catalytic stability of the Pd-Pt/*m*-GO in comparison with Pd-Pt/GO, and Pd-Pt/AC in the reduction of 2,4-

**TABLE 5** Effect of solvent

Entry	Solvent	Time (min)	Yield (%)	TOF (h <sup>-1</sup> )
1	Acetic acid	15	100	2700
2	Ethanol	15	5	135
3	Methanol	15	100	2700
4	Dichloromethane	15	-	-

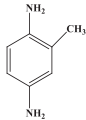
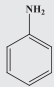
Reaction Conditions: 2,4-dinitrotoluene (5000 mg), catalyst (100 mg), P<sub>H<sub>2</sub></sub> = 0.2 MPa

**TABLE 6** Formation of aromatic amines from aromatic nitro compounds

Entry	Substrate	Product	Time (min)	Yield (%)	TOF ( $\text{h}^{-1}$ )
1	2,4-dinitrotoluene		15	100	2700
2	2-nitrotoluene		8	100	6837
3	4-nitrotoluene		6	100	9114
4	2-chloro-5-nitrotoluene		15	94	2739
5	2,6-dinitrotoluene		40	100	1013
6	3,4-dinitrotoluene		15	88	2376
7	4-chloro-2-nitro toluene		15	97	2826
8	2-methyl-4,6-dinitrophenol		15	75	1892
9	4-methyl-2,6-dinitrophenol		15	73	1842
10	2-methyl-3-nitrophenol		60	95	775
11	2,4-dinitrophenol		60	81	550
12	4-nitrophenol		40	97	1308
13	3-nitrophenol		40	90	1214
14	4-methyl-2-nitroaniline		15	88	2891

(Continues)

TABLE 6 (Continued)

Entry	Substrate	Product	Time (min)	Yield (%)	TOF (h <sup>-1</sup> )
15	2-methyl-4-nitroaniline		15	92	3023
16	Nitrobenzene		8	100	7637

Reaction Conditions: substrate (5000 mg), catalyst (100 mg), CH<sub>3</sub>OH (solvent) = 150 ml, P<sub>H<sub>2</sub></sub> = 0.2 MPa, T = 50 °C

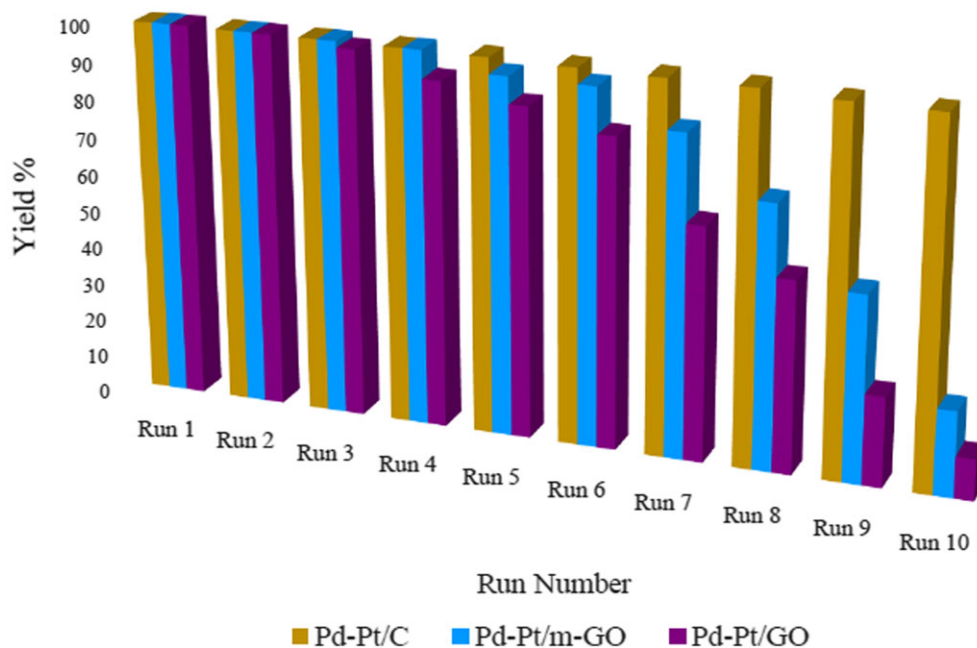


FIGURE 8 Reusability of the Pd-Pt/AC, Pd-Pt/m-GO and Pd-Pt/GO catalysts. Reaction Conditions: 2,4-dinitrotoluene (5000 mg), catalyst (100 mg, 5 w%, Pd/Pt: 7:1), CH<sub>3</sub>OH (solvent) = 150 ml, P<sub>H<sub>2</sub></sub> = 0.2 MPa, t = 15 min, T = 50 °C

dinitrotoluene is shown in Figure 8. In this regard, after each run, the catalyst was separated from the reaction mixture and washed with methanol, then by dichloromethane, and dried at 50 °C. The activity of the catalyst was almost steady after six consecutive runs; after the 7<sup>th</sup> to 10<sup>th</sup> runs, the reactivity was decreased appreciably. The reaction condition was not harsh, but leaching of the catalyst from the surface of the support was inevitable. On the basis of ICP measurements (Table 7), and in agreement with reusability data the Pd-Pt/AC catalyst has shown the best performance, and the Pd-Pt/m-GO was better than the Pd-Pt/GO catalyst. Clearly, modification of GO has improved the stability of the catalyst to some extent, but these effects do not appear to be able to counterbalance the role of better distribution of metal nanoparticles and their interactions with the activated carbon electron densities. If we realize that recovery of

the Pd-Pt/m-GO, especially in large scale, might be much more convenient, we should give a good credit to the prepared catalyst! As a final point, the data in Table 8 compares the result obtained over Pd-Pt/m-GO catalyst and other catalysts used for reduction of nitrobenzene that the catalyst introduced in this work might be one of the best catalysts.

TABLE 7 ICP analysis of the fresh and used catalysts

Entry	Catalyst	Pd (wt %)		Pt (wt %)	
		Fresh Catalyst	After 10 runs	Fresh Catalyst	After 10 runs
1	Pd-Pt/AC	4.13	2.38	0.7	0.44
2	Pd-Pt/GO	3.82	0.91	0.66	0.23
3	Pd-Pt/m-GO	3.9	1.4	0.67	0.29

**TABLE 8** hydrogenation of nitrobenzene to aniline with different catalysts

Entry	Catalyst	H <sub>2</sub> (MPa)	Solvent	T (°C)	Substrate	Product	Time (min)	Yield (%)	Ref
1	Montmorillonite Sialamine Palladium (II) Complex	0.1	EtOH	135	Nitrobenzene	Aniline	5–10	98	[16]
2	RuCl <sub>2</sub> (PPh) <sub>3</sub>	8	Benzene:EtOH (1:1)	125	Nitrobenzene	Aniline	420	90	[14]
3	Fe (CO)(PPh <sub>3</sub> ) <sub>2</sub>	8	Benzene:EtOH (1:1)	125	Nitrobenzene	Aniline	480	87	[14]
4	Pt/RGO	1	EtOH	20	Nitrobenzene	Aniline	20	99.1	[12]
5	Ru (II)Phenanthroline Complex	2.75	H <sub>2</sub> O	160	Nitrobenzene	Aniline	60	99.5	[18]
6	FeSO <sub>4</sub> ·7H <sub>2</sub> O	2.75	H <sub>2</sub> O	150	Nitrobenzene	Aniline	144	98.5	[34]
7	Pt/TiO <sub>2</sub> /RGO	4	-	-	Nitrobenzene	Aniline	480	99.9	[3]
8	MCM-Silylamine Palladium (II)	0.1	THF	-	Nitrobenzene	Aniline	360	100	[11]
9	PVP-Pd/Pt	0.1	EtOH, H <sub>2</sub> O	65	Nitrobenzene	Aniline	14	>99	[19]
10	Pt/CNT	0.1	Alcohol	-	Nitrobenzene	Aniline	40	90	[2]
11	Fe <sub>2</sub> P@C	5	H <sub>2</sub> O:THF (1:1)	120	Nitrobenzene	Aniline	720	>99	[35]
12	Pd-Pt/ <i>m</i> -GO	0.2	MeOH	50	Nitrobenzene	Aniline	8	100	This work

## 4 | CONCLUSIONS

To summarize, a new heterogeneous nano-catalyst, i.e., Pd-Pt/*m*-GO, was prepared and characterized using different techniques. The catalyst could catalyze the reduction of a variety of nitro arenes in a short time which could be economically feasible. Under the optimized conditions, 50 °C, P<sub>H<sub>2</sub></sub> = 0.2 MPa, 15 min, the catalyst reduced 2,4-dinitrotoluene, an industrially important raw material, quantitatively with 100% selectivity.

## ACKNOWLEDGMENTS

We sincerely thank the Isfahan University of Technology and Karoon Petrochemical Company for their support and assistance in this project.

## ORCID

Mehran Ghiaci  <https://orcid.org/0000-0002-0686-7778>

## REFERENCES

- [1] R. Downing, P. Kunkeler, H. Van Bekkum, *Catal. Today* **1997**, 37, 121.
- [2] C.-H. Li, Z.-X. Yu, K.-F. Yao, S.-f. Ji, J. Liang, *J. Mol. Catal. A: Chem.* **2005**, 226, 101.
- [3] Y. Zhao, H. Zhang, C. Huang, S. Chen, Z. Liu, *J. Colloid Interface Sci.* **2012**, 374, 83.
- [4] H.-U. Blaser, *Science-New York Then Washington* **2006**, 313, 312.
- [5] A. M. Tafesh, J. Weiguny, *Chem. Rev.* **1996**, 2035, 96.
- [6] P. Zhou, D. Li, S. Jin, S. Chen, Z. Zhang, *Int. J. Hydrogen Energy* **2016**, 41, 15218.
- [7] P. Sangeetha, K. Shanthi, K. R. Rao, B. Viswanathan, P. Selvam, *Appl. Catal. A. Gen.* **2009**, 353, 160.
- [8] Y.-S. Feng, J.-J. Ma, Y.-M. Kang, H.-J. Xu, *Tetrahedron* **2014**, 70, 6100.
- [9] H. Göksu, S. F. Ho, O.n. Metin, K. Korkmaz, A. Mendoza Garcia, M. S. Gültekin, S. Sun, *ACS Catal.* **2014**, 4, 1777.
- [10] G. He, W. Liu, X. Sun, Q. Chen, X. Wang, H. Chen, *Mater. Res. Bull.* **2013**, 48, 1885.
- [11] M. L. Kantam, T. Bandyopadhyay, A. Rahman, N. M. Reddy, B. Choudary, *J. Mol. Catal. A: Chem.* **1998**, 133, 293.
- [12] R. Nie, J. Wang, L. Wang, Y. Qin, P. Chen, Z. Hou, *Carbon* **2012**, 50, 586.
- [13] A. Rahman, S. Jonnalagadda, *Catal. Lett.* **2008**, 123, 264.
- [14] J. Knifton, *J. Org. Chem.* **1976**, 41, 1200.
- [15] A. Saha, B. Ranu, *J. Org. Chem.* **2008**, 73, 6867.
- [16] K. Mukkanti, Y. S. Rao, B. Choudary, *Tetrahedron Lett.* **1989**, 30, 251.
- [17] R. G. de Noronha, C. C. Romao, A. C. Fernandes, *J. Org. Chem.* **2009**, 74, 6960.
- [18] A. A. Deshmukh, A. K. Prashar, A. K. Kinage, R. Kumar, R. Meijboom, *Ind. Eng. Chem. Res.* **2010**, 49, 12180.
- [19] Z. Yu, S. Liao, Y. Xu, B. Yang, D. Yu, *J. Mol. Catal. A: Chem.* **1997**, 120, 247.



- [20] M. Nasrollahzadeh, S. M. Sajadi, A. Rostami-Vartooni, M. Alizadeh, M. Bagherzadeh, *J. Colloid Interface Sci.* **2016**, *466*, 360.
- [21] H. Li, S. Gan, D. Han, W. Ma, B. Cai, W. Zhang, Q. Zhang, L. Niu, *J. Mater. Chem. A* **2014**, *2*, 3461.
- [22] D. Chen, H. Feng, J. Li, *Chem. Rev.* **2012**, *112*, 6027.
- [23] D. R. Dreyer, S. Park, C. W. Bielawski, R. S. Ruoff, *Chem. Soc. Rev.* **2010**, *39*, 228.
- [24] S. Yang, J. Dong, Z. Yao, C. Shen, X. Shi, Y. Tian, S. Lin, X. Zhang, *Sci. Rep.* **2014**, *4*, 4501.
- [25] M. M. Raju, D. K. Pattanayak, *RSC Adv.* **2015**, *5*, 59541.
- [26] J. Sun, Y. Fu, G. He, X. Sun, X. Wang, *Catal. Sci. Technol.* **2014**, *4*, 1742.
- [27] C. Xu, L. Cheng, P. Shen, Y. Liu, *Electrochem. Commun.* **2007**, *9*, 997.
- [28] Z.-x. Cai, C.-c. Liu, G.-h. Wu, X.-m. Chen, X. Chen, *Electrochim. Acta* **2014**, *127*, 377.
- [29] Y. Kim, Y. Noh, E. J. Lim, S. Lee, S. M. Choi, W. B. Kim, *J. Mater. Chem. A* **2014**, *2*, 6976.
- [30] Y. Zhu, S. Murali, W. Cai, X. Li, J. W. Suk, J. R. Potts, R. S. Ruoff, *Adv. Mater.* **2010**, *22*, 3906.
- [31] U. Saha, R. Jaiswal, J. P. Singh, T. H. Goswami, *J. Nanopart. Res.* **2014**, *16*, 2404.
- [32] H. Zhao, L. Wu, Z. Zhou, L. Zhang, H. Chen, *Phys. Chem. Chem. Phys.* **2013**, *15*, 9084.
- [33] M. Tran, A. Whale, S. Padalkar, *Sensors* **2018**, *18*, 147.
- [34] R. M. Deshpande, A. N. Mahajan, M. M. Diwakar, P. S. Ozarde, R. Chaudhari, *J. Org. Chem.* **2004**, *69*, 4835.
- [35] Y. Zhu, S. Yang, C. Cao, W. Song, L.-J. Wan, *Inorg. Chem. Front.* **2018**, *5*, 1094.

## SUPPORTING INFORMATION

Additional supporting information may be found online in the Supporting Information section at the end of the article.

**How to cite this article:** Salahshournia H, Ghiaci M. Pd-Pt/modified GO as an efficient and selective heterogeneous catalyst for the reduction of nitroaromatic compounds to amino aromatic compounds by the hydrogen source. *Appl Organometal Chem.* 2019;e4832. <https://doi.org/10.1002/aoc.4832>